Inorg. Chem. **2009**, *48*, 2818−2829

Contrasts between the Vibronic Contributions in the *tris*-(2,2′-bipyridyl)Osmium(II) Emission Spectrum and the Implications of Resonance-Raman Parameters

Onduru S. Ondongo and John F. Endicott*

Department of Chemistry, Wayne State University, Detroit, Michigan 48202

Received August 8, 2008

The emission spectrum of the *tris*-(2,2′-bipyridine)osmium(II) metal-to-ligand charge transfer (MLCT) excited-state frozen solution at 77 K differs qualitatively from that expected based on its reported resonance-Raman (rR) parameters in that (1) the dominant vibronic contributions to the emission spectrum are in the low frequency regime (corresponding to nuclear displacements in largely to metal−ligand vibrational modes) and these contributions are negligible in the rR; and (2) the amplitude of the emission sideband components that correspond to envelopes of largely bpy centered vibrational modes is about 40% of that expected (relative to the amplitude observed for the band origin) for a simple vibronic progression in these modes. The distortions in low frequency vibrational modes are attributable to configurational mixing between metal centered (LF) and MLCT excited states, and the small amplitudes of the bpy-mode vibronic components may be a consequence of some intrinsic differences of the distortions of the ^{3}MLCT and ^{1}MLCT excited states such as the zero-field splitting of the ^{3}MLCT excited state and the different distortions of these excited-state components.

Introduction

The reactivity of transition metal complex excited states is of considerable interest in a number of contexts,[1−6] and it is expected to be a function of the excited-state energy and molecular structure. The reactive electronic excited states of transition metals are often the lowest energy excited states with spin multiplicities which generally differ from those of the ground state, and structural information about them is very difficult to obtain. Experimental emission spectra contain information about excited-state energies (in a contribution from a band origin component $I_{\nu_m(0'0)}$) and excited-state molecular structure (in a vibronic sideband contribution) and observations on these spectral contributions for $[Ru(L)_{6-2n}(bpy)_n]^{2+7-9}$ complexes are conveniently represented as a function of the emission frequency, ν_m,[10]

$$I_{\nu_m(\exp t)} \cong \nu_m^3 M_{eg}^2 B(A_{\nu_m(0'0)} + V_{\nu_m}) \quad (1)$$

where M_{eg} is the transition dipole, V_{ν_m} is a function that represents the shape of the envelope of vibronic contributions to the emission spectrum, and $I_{\nu_m(0'0)} = \nu_m C G_{(0'0)}/\gamma$; B and C are different collections of physical constants (see the Experimental Section below) and $I_{\nu_m(0'0)}$ is assumed to have a Gaussian band shape, $G_{(0'0)}$. While the distortion amplitudes inferred from resonance-Raman (rR) spectra are among the most important experimental means for characterizing the transition metal-to-ligand-charge-transfer (MLCT) excited-state structures,[11−13] the excited states probed by rR spectra are the Franck−Condon excited states generated by spin allowed electronic transitions from the ground state (^{1}MLCT in the cases considered here), while the reactive and emitting

* To whom correspondence should be addressed. E-mail: jfe@chem.wayne.edu.

(1) Gratzel, M. *Inorg. Chem.* **2005**, *44*, 6841.
(2) Fujita, E. *Coord. Chem. Rev.* **1999**, *186*, 373.
(3) Hagfeldt, A.; Gratzel, M. *Acc. Chem. Res.* **2000**, *33*, 269.
(4) Lewis, N. S. *J. Electroanal. Chem.* **2001**, *508*, 1.
(5) Lewis, N. S. *Inorg. Chem.* **2005**, *44*, 6900.
(6) Meyer, G. J. *Inorg. Chem.* **2005**, *44*, 6802.
(7) Chen, Y.-J.; Xie, P.; Heeg, M. J.; Endicott, J. F. *Inorg. Chem.* **2006**, *45*, 6282.
(8) Odongo, O. S.; Heeg, M. J.; Chen, J. Y.; Xie, P.; Endicott, J. F. *Inorg. Chem.* **2008**, *47*, 7493.
(9) Xie, P.; Chen, Y.-J.; Uddin, M. J.; Endicott, J. F. *J. Phys. Chem. A* **2005**, *109*, 4671.
(10) Birks, J. B. *Photophysics of Aromatic Molecules*; Wiley-Interscience: New York, 1970.
(11) Myers, A. B. *Chem. Phys.* **1994**, *180*, 215.
(12) Myers, A. B. In *Laser Techniques in Chemistry*; Myers, A. B., Rizzo, T. R., Eds.; John Wiley & Sons, Inc., 1995; Vol. XXIII, p 325.
(13) Myers, A. B. *Acc. Chem. Res.* **1997**, *30*, 519.

10.1021/ic801512g CCC: $40.75
Published on Web 02/24/2009

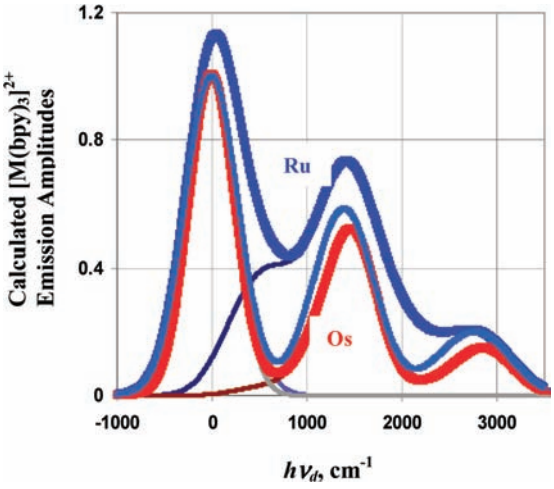

Figure 1. Calculated emission spectra of $[Ru(bpy)_3]^{2+}$ (blue) and $[Os(bpy)_3]^{2+}$ (red) based on the $I_{\nu_m(f)}$ components (blue-gray and gray Gaussian curves) deconvoluted from the 77 K emission spectra and the envelope of vibronic components (1st and 2nd order terms only) which are based on the reported rR parameters and the bandwidth of $I_{\nu_m(f)}$. The $I_{\nu_m(f)}$ components are centered at $\nu_d = 0$ with $I_{max(f)} = 1.00$. The dark blue and dark red curves are the respective sums of 1st and 2nd order, rR-based vibronic components; the light blue curve is the calculated $[Ru(bpy)_3]^{2+}$ emission spectrum without any contribution from low frequency vibrational modes and assuming that $\gamma = 1.0$.

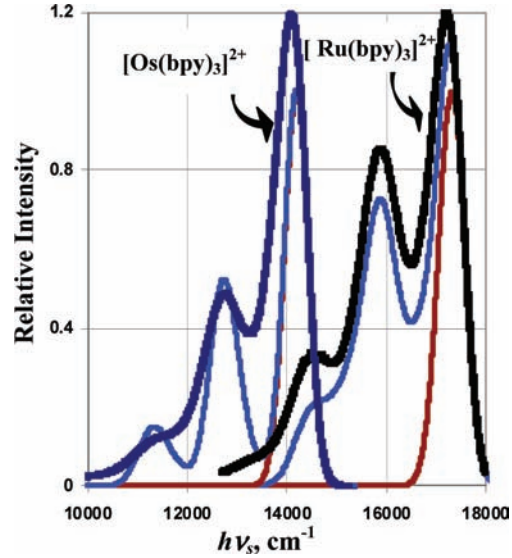

Figure 2. Comparison of the emission spectra observed for $[Os(bpy)_3]^{2+}$ (dark blue on the left) and $[Ru(bpy)_3]^{2+}$ (black on the right) to the spectra calculated using rR parameters reported for each complex (blue curves). The fundamental components (dark red Gaussians) have been iteratively optimized (adjusting amplitudes and bandwidths) to minimize the overall deviations between the observed and calculated spectra. The fits of rR parameters are based on eq 1 with $\gamma = 1.0$.

excited states are generally vibrationally equilibrated and have spin multiplicities different from those of the ground states (^{3}MLCT). However, in the simple limit in which the distortions in the ^{1}MLCT and ^{3}MLCT excited states are in the same vibrational modes and in the absence of perturbations such as configurational mixing with other electronic states or spin−orbit coupling, V_{ν_m} and the scaling factor, γ, should be the same for the two excited states. Configurational mixing and spin−orbit coupling can have significant effects on the observations in the actual systems: (1) configurational mixing between the MLCT excited states and the ground state is expected to reduce the excited-state distortion;[9,14] and (2) spin−orbit coupling will split the excited states with triplet spin multiplicity into several excited-state components each of which may have different distortions, extents of configurational mixing, and so forth.

We have used a best fit Gaussian (designated as the "fundamental" component, $I_{\nu_m(f)}$) as an estimate of $I_{\nu_m(0'0)}$ and found that, with respect to this component, the emission bandshapes of $[Ru(bpy)_3]^{2+}$ and $[Ru(NH_3)_4bpy]^{2+}$ are well reproduced by their respective rR parameters (using Gaussian vibronic band shape components and the $I_{\nu_m(f)}$ bandwidths) for $\gamma \approx 1.0$.[7−9] The same approach applied to the $[Os(bpy)_3]^{2+}$ emission is reported here and implies a smaller value of γ and has led to an examination of the implications of the experimental band shape correlations.

The rR parameters reported for the $[Os(bpy)_3]^{2+}$ complex differ from those of the Ru-bpy complexes in the absence of appreciable vibronic contributions in the low frequency regime (largely metal−ligand vibrational modes with $h\nu_{lf} <$ 1000 cm^{-1}; see Figure 1). This suggests that[8] the $[Os(bpy)_3]^{2+}$ rR parameters can be used to model those V_{ν_m} contributions which arise predominately from distortions in the bpy vibrational modes of MLCT excited states, assuming that V_{ν_m} for these complexes can be approximately resolved into contributions that arise from identifiable functional groups[8]

$$V_{\nu_m} \approx A_{\nu_m(bpy)} + A_{\nu_m(ML)} + A_{\nu_m(OT)} \quad (2)$$

Each of the terms in eq 2 represents the envelope of overlapping vibronic progressions ($j = 1, 2,...$) in all of the relevant molecular vibrational modes, k, for the different functional groups (e.g., with $s = ML$ or bpy), and

$$A_{\nu_m(s)} = \sum_k A_{\nu_m(k)} = \sum_k \left(\sum_j A_{\nu_m(0'j)} \right)_k \quad (3)$$

The $A_{\nu_m(OT)}$ term contains spectral sideband contributions other than those that can be attributed to distortions in predominately bpy or metal−ligand vibrational modes; this includes contributions such as those of low frequency/medium frequency combination bands, as well as contributions from other functional groups.

The rR parameters reported for $[Ru(bpy)_3]^{2+}$[15] and $[Ru(NH_3)_4bpy]^{2+}$[16] implicate larger distortions in the metal−ligand vibrational modes than is expected for a simple electron transfer process,[17] but they are consistent with significant configurational mixing of the LF and MLCT

(14) Seneviratne, D. S.; Uddin, M. J.; Swayambunathan, V.; Schlegel, H. B.; Endicott, J. F. *Inorg. Chem.* **2002**, *41*, 1502.
(15) Maruszewski, K.; Bajdor, K.; Strommen, D. P.; Kincaid, J. R. *J. Phys. Chem.* **1995**, *99*, 6286.
(16) Hupp, J. T.; Williams, R. T. *Acc. Chem. Res.* **2001**, *34*, 808.
(17) Endicott, J. F. In *Comprehensive Coordination Chemistry II*, 2nd ed.; McCleverty, J., Meyer, T. J., Eds.; Pergamon: Oxford, U.K., 2003; Vol. 7; p 657.

excited states.[8,9,17−19] The much smaller rR-based distortions in the low frequency vibrational modes of $[Os(bpy)_3]^{2+}$[20] (see Figure 1) suggest that there is very little LF/MLCT configurational mixing in its Franck−Condon-MLCT excited state. That the spectra based on the $[Ru(bpy)_3]^{2+}$ and $[Os(bpy)_3]^{2+}$ rR parameters are very similar when the low frequency vibronic contributions are not included for the former (light blue curve in Figure 1) indicates that the distortions in bpy vibrational modes of the Franck−Condon ^{1}MLCT excited states of these two complexes are comparable. However, early work with the $[Os(bpy)_3]^{2+}$ complex implicated low frequency vibronic contributions to the ambient emission,[21] and the small ^{1}MLCT excited-state distortions in the low frequency regime implicated by the rR parameters indicate that even moderate configurational mixing between the ^{3}LF and ^{3}MLCT excited states should be clearly manifested by a dramatic enhancement of low frequency vibronic contributions in the emission. The $[Os(bpy)_3]^{2+}$ emission spectra in frozen solution at 77 K that are reported here do have large contributions from low frequency vibronic components but smaller medium frequency vibronic components than are expected based on the reported rR parameters. These observations demonstrate that there are important differences in the excited-state distortions within the singlet and triplet manifolds of these complexes.

Experimental Section

Materials. The starting materials K_2OsCl_6 and $(NH_4)_2OsCl_6$ were purchased from Strem Chemicals and used as received. $Os(bpy)_2Cl_2.2H_2O$ was prepared following a standard protocol.[22] $[Os(h_8\text{-bpy})_{3-n}(d_8\text{-bpy})_n]^{2+}$ complexes ($n = 0-3$) were prepared according to the literature procedures;[23] more details are in the Supporting Information S2.[24] Samples of $[Ru(bpy)_3](PF_6)_2$ were prepared and purified as described previously.[9]

Instrumentation. The emission spectrometer, its calibration, and spectral acquisition procedures have been described in detail elsewhere.[9,25] All emission spectra were obtained in 77 K glasses. The emission of the $[Os(bpy)_3]^{2+}$ complex occurs in a relatively insensitive region (~10,000−14,000 cm^{-1}) for detection with the OMA V, and second order dispersion of this emission would fall outside of our detection range. Consequently, we have used the first order dispersion and very careful calibrations of the spectrometer response for this complex. We have used second order dispersion of the $[Ru(bpy)_3]^{2+}$ emission as described previously; there is some instrumental noise at ~1400 nm in the resulting emission spectra.[9] The complexes were irradiated in their MLCT absorption bands using a 532 nm (50 mW) CW diode MGL-S-B 50mW laser module (Changchun Industries Optoelectronics Tech Co. Ltd.) purchased from OnPoint Lasers Inc. ASCII files were transferred to Excel, and 10 or more spectra were averaged for each complex.

UV−visible spectra were recorded using a Shimadzu UV-2101PC spectrophotometer; ^{1}H and ^{13}C NMR spectra were obtained using a Varian 300 MHz instrument. The absorption spectra are presented in Supporting Information Figure S3.[24]

Cyclic voltammograms (CV) were obtained in dry CH_3CN using a three-electrode system consisting of a Ag/AgCl reference electrode, a Pt wire counter electrode, and a Pt disk working electrode with a BAS model 100A electrochemical workstation for measurements. The solutions consisted of the complex dissolved in acetonitrile containing 0.1 mol/L tetrabutylammonium hexafluorophosphate as electrolyte. Ferrocene was dissolved in the sample solutions as an internal reference for the CV. The electrochemical observations are summarized in Supporting Information S4.[24]

Methods Used for the rR Fittings. 1. General Procedures. The emission spectrum of a complex is represented as the sum of the intensities contributed by the radiative decay of an electronic excited state to vibrational modes of the ground state. The component intensities are determined by the differences in the molecular and electronic structures of the ground and excited states: (a) the vibrational quanta ($h\nu_k$) of the mode k; (b) the square of the displacements of the excited-state potential energy (PE) minimum in the normal coordinates of that mode (represented by a vibrational reorganizational energy, λ_k); (c) symmetry constraints on the electronic or vibronic transitions (contained in the electronic matrix element H_{ij}).

When the ground- and excited state differ in geometry only in the coordinates of a single normal mode k of the ground state and for Gaussian component bandshapes,[11,13,26,27]

$$\left(I_{\nu_m(\exp t)}\right)_k = \nu_m C \sum_j F_{j,k}[\exp\{-(4g_{j,k}{}^2 \ln 2)/\Delta\nu_{1/2}{}^2\}] \quad (4)$$

where

$$C = \frac{64\pi^4}{3h^3c^3 \ln 10} \frac{\eta^3 H_{eg}^2 (\Delta\mu_{eg})^2}{(4\pi\lambda_s k_B T)^{1/2}} \quad (5)$$

$$F_{j,k} = \frac{S_k^j e^{-S_k}}{j!} \qquad S_k = \frac{\lambda_k}{h\nu_k} \quad (6)$$

$$g_{j,k} = E_{eg}^{0'0} - \lambda_s - jh\nu_k - h\nu_m \quad (7)$$

In these equations, η is the index of refraction, ν_m is the frequency of the incident radiation, $\Delta\mu_{eg}$ is the difference between the excited-state and ground-state dipole moments ($H_{eg}/h\nu_{eg}\,\Delta\mu_{eg} \approx M_{eg}$),[12,27,28] λ_s is the combination of the reorganizational energies of the solvent and other displacement modes with $h\nu_s < 4k_BT$, and c is the speed of light. The component with $j = 0$ corresponds to the transition between the PE minima of the two states, {e,0′}→{g,0}, with an intensity that can be represented as $I_{\nu_m(0'0)}$, where

$$I_{\nu_m(0'0)} \cong I_{\max(0'0)} \exp\{-[E_{eg}^{0'0} - h\nu_m]^2/(\Delta\nu_{1/2}{}^2/4 \ln 2)\} \quad (8)$$

The largest amplitude contribution to the emission spectra of these $[M(L)_4bpy]^{m+}$ complexes has been attributed to this component.[9,18,19] Distortions in a large number (>11) of different

(18) Endicott, J. F.; Chen, Y.-J. *Coord. Chem. Rev.* **2007**, *251*, 328.
(19) Endicott, J. F.; Chen, Y.-J.; Xie, P. *Coord. Chem. Rev.* **2005**, *249*, 343.
(20) Thompson, D. G.; Schoonover, J. R.; Timpson, C. J.; Meyer, T. J. *J. Phys. Chem. A* **2003**, *107*, 10250.
(21) Casper, J. V.; Kober, E. M.; Sullivan, B. P.; Meyer, T. J. *J. Am. Chem. Soc.* **1982**, *104*, 630.
(22) Buckingham, D. A.; Dwyer, F. P.; Goodwin, H. A.; Sargeson, A. M. *Aust. J. Chem.* **1964**, *17*, 325.
(23) Kober, M. E.; Caspar, J. V.; Sullivan, B. P.; Meyer, T. J. *Inorg. Chem.* **1988**, *27*, 4587.
(24) Supporting Information, see the paragraph at the end of this paper.
(25) Chen, Y.-J.; Xie, P.; Endicott, J. F. *J. Phys. Chem. A* **2004**, *108*, 5041.
(26) Englman, R.; Jortner, J. *Mol. Phys.* **1970**, *18*, 145.
(27) Gould, I. R.; Noukakis, D.; Gomez-Jahn, L.; Young, R. H.; Goodman, J. L.; Farid, S. *Chem. Phys.* **1993**, *176*, 439.
(28) Mulliken, R. S.; Person, W. B. *Molecular Complexes*; Wiley-Interscience: New York, 1967.

vibrational modes typically contribute to the emission bandshapes,[15,16,20,29] and these contributions are not generally resolved in the 77 K emission spectra so we have evolved systematic approaches for evaluating the contributions of the envelopes of vibronic contributions in the low frequency (mostly metal−ligand) and the medium frequency (mostly bpy) regimes of vibrational modes (i.e., as in eq 2).[8,9]

2. Evaluation of the {e,0′}→{g,0} Contribution to the Emission Spectra. Since this contribution is not resolved in the 77 K emission spectra, we generally determine a "fundamental emission component,"[7−9] $I_{\nu_m(f)}$, by means of a careful fitting of a Gaussian component to the high energy, dominant emission peak using Grams32, and this is further optimized to minimize deviations from the observed emission on its high energy side.[8,9] In the present study, we have modified this procedure by using an iterative fitting of the fundamental and vibronic components based on the reported rR parameters (adjusting $I_{\max(f)}$ and $\Delta\nu_{1/2}$ of $I_{\nu_m(f)}$) to the spectra of the $[Ru(h_8\text{-bpy})_3]^{2+}$ and $[Ru(d_8\text{-bpy})_3]^{2+}$ complexes. In the limit that $I_{\nu_m(0'0)}$ dominates the emission spectrum and/or there is very little overlap with vibronic components, $I_{\nu_m(f)} = I_{\nu_m(0'0)}$.

3. Spectral Envelope of Vibronic Contributions: The Difference Spectrum. The $I_{\nu_m(f)}$ and $\gamma C A_{\nu_m(bpy)}$ contributions (eqs 1, 2, and 5) appear to be dominant features of the emission spectra of the complexes considered here. We have based the evaluation of the $A_{\nu_m(bpy)}$ component on the reported rR parameters[15,20] as described elsewhere;[8] however, some of the observations reported here, and more generally the simplicity of the experimental band shape fittings[7−9,18,19] raise issues about the interpretation of γ and about the $I_{\nu_m(f)}$ component that is deconvoluted from the observed spectrum; these issues are considered in the Discussion section below (see also Supporting Information S5).[24] The removal of the {e,0′}→{g,0} component contribution from the observed emission spectrum results in the emission sideband which is the convolution of the vibronic progressions in each of the k distortion modes (eq 4) plus the combination bands containing contributions from different first order vibrational modes. Thus, on the basis of eqs 1 and 5 with $I_{\nu_m} = \nu_m^{-1} I_{\nu_m(\exp\ t)}$, the experimental difference spectrum is

$$A_{\nu_m(diff)} = \frac{I_{\nu_m} - I_{\nu_m(f)}}{C} \tag{9}$$

The vibronic components that contribute to $A_{\nu_m(diff)}$ can be organized in various ways,[8,9] and here we consider the intensity contribution of the kth distortion mode to be the sum over all components j of the corresponding vibronic progression so that the emission intensity at a frequency ν_m is given by the sum of all of the progressions in the distortion modes plus the intensity contributions of combination bands (p,q; p,q,r; etc.),[9]

$$(I_{\nu_m} - I_{\nu_m(0'0)}) \cong \sum_k I_{\nu_{m(k)}} + \sum_{p,q} I_{\nu_{m(p,q)}} + \sum_{p,q,r} I_{\nu_{m(p,q,r)}} + \ldots \tag{10}$$

Even in the relatively broadband emission spectra obtained at 77 K, the envelopes of vibronic contributions in different spectral regions are often clearly displayed in the difference spectra or in the differences in emission bandshapes for the isotopomers of some complexes.[7−9]

4. Evaluation of the Envelopes of Vibronic Components. The rR spectra of these complexes indicate that their excited states are distorted in more than 11 vibrational modes, and the frequencies of these distortion modes are comparable for the $[Ru(bpy)_3]^{2+}$, $[Ru(NH_3)bpy]^{2+}$, and $[Os(bpy)_3]^{2+}$ complexes although there are large contrasts in the amplitudes of contributions in different spectral regions for these complexes, see Figure 1 and Supporting Information S1.[8,15,16,20,24] The procedure for constructing a calculated emission or difference spectrum from these rR parameters has been discussed in detail[8,9] and is summarized in Supporting Information S6.[24] In the present report iterative fittings of $I_{\nu_m(f)}$ and V_{ν_m}, constructed from the rR parameters of the different complexes, have been used in the evaluation of the respective $A_{\nu_m(bpy)}$ contributions.

The 77 K emission bandshapes of most $[Ru(L)_{6-2n}(bpy)_n]^{2+}$ complexes implicate contributions in the low frequency regime ($\nu_k < 1000\ cm^{-1}$) which are attributable to distortions in metal−ligand vibrational modes.[7,8] To systematically assess these contributions it is necessary to remove the contributions of the bpy distortion modes from $A_{\nu_m(diff)}$ to obtain a "remainder" spectrum, $A_{\nu_m(rem)} \cong A_{\nu_m(diff)} - A_{\nu_m(bpy)}$.[8] We have evaluated variations in $A_{\nu_m(lf)} \approx A_{\nu_m(ML)}$ using an empirical fitting of the remainder spectrum that amounts to attributing the low frequency vibronic envelopes (designated by the *lf* subscript) to distortions in a single "equivalent" vibrational mode. However, such single mode representations of the envelopes that arise from the convolution of several vibronic components must be interpreted with caution partly because their amplitudes are strong functions of the component bandwidth and cannot be simply interpreted in terms of excited-state distortions and partly because the details (such as amplitude and bandwidth) of the vibronic envelopes may be different depending on whether they originate from the distortions of the diabatic MLCT excited state or from configurational mixing with another state (see the discussion of some of these issues below). The bandwidth contributions will at least partly cancel in ratios of vibronic envelopes such as $[A_{\max(lf)}/A_{\max(bpy)}]$. For purposes of comparison of the relative significance of the different vibronic contributions one can either use the corresponding difference spectrum amplitudes or construct empirical "progressions", $A_{\nu_m(lf1)}$, in $G_{\nu_m(lf)}$ and its combinations with bpy modes (b) obtained from the rR parameters (note that for simplicity, the pre-exponential coefficients are not specified here),[8]

$$A_{\nu_m(lf1)} = G_{\nu_m(lf)} + G_{\nu_m(lf2)} + G_{\nu_m(lf3)} + G_{\nu_m(lf^*b)} + G_{\nu_m(lf2^*b)} + G_{\nu_m(lf^*b2)} \tag{11}$$

The Gaussian functions in eq 11 are constructed for a best fit of the remainder spectrum by adjusting $h\nu_{\max(lf)}$, $\Delta\nu_{1/2(lf)}$, and $A_{\max(lf)}$ of the $G_{\nu_m(lf)}$ component; the higher order terms so generated approximate a vibronic "progression" in the *lf* mode and they are based on a best fit to the envelope of rR-based low frequency components for $[Ru(NH_3)_4bpy]^{2+}$, but they do not correspond to a vibronic progression in a single mode as in eqs 4−7.[8] The intergroup combination band contributions (designated by * in the subscript) are based on a Gaussian fit, $G_{\nu_m(lf)}$ (with $h\nu_{\max(B)}$, $\Delta\nu_{1/2(B)}$, and $I_{\max(B)}$) to the envelope of first order rR-based medium frequency (*mf*) vibronic contributions for the complex. The combination band amplitudes are useful in assessing the significance

(29) Yersin, H.; Braun, D.; Hensler, G.; Galhuber, E. In *Vibronic Processes in Inorganic Chemistry*; Flint, C. D., Ed.; Kluwer: Dordrecht, 1989; p 195.
(30) Curtis, J. C.; Sullivan, B. P.; Meyer, T. J. *Inorg. Chem.* **1983**, *22*, 224.
(31) Lever, A. B. P.; Dodsworth, E. In *Electronic Structure and Spectroscopy of Inorganic Compounds*; Lever, A. B. P., Solomon, E. I., Eds.; Wiley: New York, 1999; Vol. II, p 227.

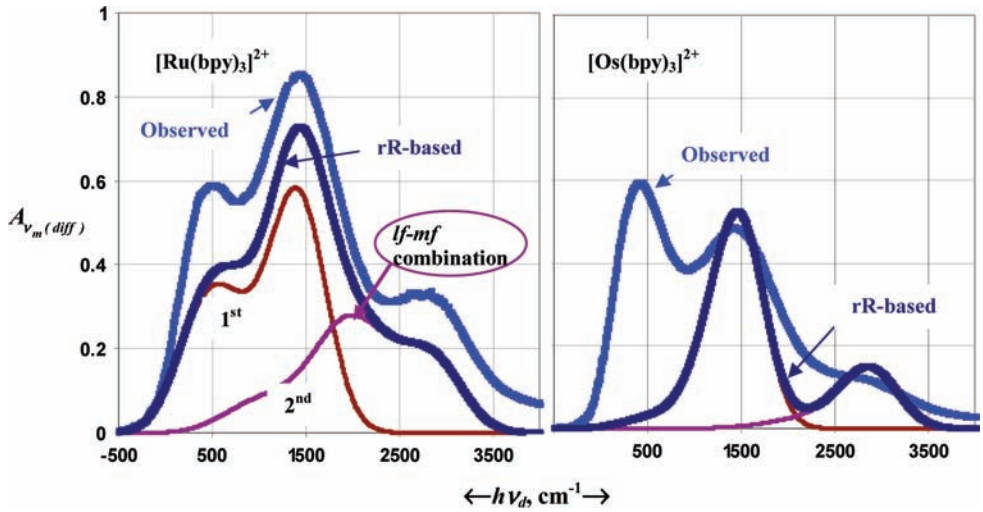

Figure 3. Comparison of the observed difference spectra (blue) to the sum of the attenuated rR-based vibronic components (dark blue) for $[Ru(bpy)_3]^{2+}$ [15] (left panel) and $[Os(bpy)_3]^{2+}$ [20] (right panel). The 1st (dark red) and 2nd (violet) vibronic components and included, but third and higher order components have not been calculated. The envelopes of 1st, 2nd order (including low frequency-medium frequency intergroup combination band) vibronic contributions are noted in the left panel. The fits of rR parameters are based on eq 1 with $\gamma = 1.0$.

of low frequency vibronic contributions. Further details can be found in the Supporting Information S6.[24]

5. Basis for Correlation of Spectral and Electrochemical Parameters. While the electrochemical and optical transition energies of a linked D−A couple are related, they differ by entropy contributions and the electron transfer equilibrium of a linked donor (D)-acceptor (A) complex,[14,30−32]

$$D^+\text{-}A + D\text{-}A^- \rightleftarrows D\text{-}A + D^+\text{-}A^-, \quad K_{DA} \qquad (12)$$

The D^+-A^- species represents the vibrationally equilibrated electronic excited state (at its PE minimum) and differs in energy from the Franck−Condon excited state by λ_e, and the half-wave potentials of the D-A/D-A^- and D^+-A/D-A couples differ from those of the independent A/A^- and D^+/D couples by approximately the ground-state stabilization energy, ε_{ge} (note the sign convention: $\varepsilon_{ge} < 0$). Then, for ε_{eg} the excited-state destabilization energy at its PE minimum, $RT(\ln K_{DA}) \cong (\varepsilon_{eg} - \varepsilon_{ge})$ and K_{el} represents purely electrostatic contributions, the vertical ground state to Franck−Condon excited-state transition (for $\alpha_{ge}^2 < 0.1$ and $\lambda_e \cong \lambda_g = \lambda$; K_{exch} is the electron exchange integral; see also Supporting Information S7)[24] can be represented as

$$h\nu_{max(abs)} \cong E_{ge}^{00'} + \lambda_e \cong -F\Delta E_{1/2} - \varepsilon_{ge} + \varepsilon_{eg} + \lambda_e + Y \qquad (13)$$

$$h\nu_{max(em)} \cong -F\Delta E_{1/2} - \varepsilon_{ge} + \varepsilon_{eg} - \lambda_e - 2K_{exch} + Y \qquad (14)$$

where $Y = RT(\ln K_{el}) + T\Delta S$ should be similar for the $[M(bpy)_3]^{2+}$ complexes.

Results

A. Emission Spectra of the $[Os(bpy)_3]^{2+}$ h/d Isotopomers. The medium frequency vibronic sidebands of these spectra (with maxima at $h\nu_d \sim 1400-1500$ cm^{-1}) are weaker than expected on the basis of the reported rR parameters (i.e., as shown in Figure 1). This contrast is clear from the comparison of the experimental spectra to the calculated spectra in Figure 2 (see also Figure 1).

We have iteratively optimized the fits between the observed and calculated emission spectra in Figure 2 by varying $I_{max(f)}$ and $\Delta\nu_{1/2}$ while holding the values of S_k constant and assuming eq 1 with $\gamma = 1.0$; however, this was very difficult for the $[Os(bpy)_3]^{2+}$ spectrum because of the very large amplitude of the low frequency vibronic contributions, and we were unable to find, within the stated constraints, any fit in which the amplitude of the vibronic envelope calculated from rR parameters was always smaller than or equal to the observed spectral amplitude. In contrast, the spectrum calculated for $[Ru(bpy)_3]^{2+}$, based on the same assumptions, was always smaller in amplitude than the observed spectrum, which is expected based on eq 1 (with $\gamma = 1.0$) since (1) the rR parameters for this complex[15] seem to underestimate the amplitude of the envelope of low frequency contributions found in the emission;[8,9] and (2) we have not included any vibronic contributions of order greater than two. Thus, the $[Ru(bpy)_3]^{2+}$ spectrum is fitted reasonably well if it is assumed that the low frequency distortions in its emitting excited state are greater than those in its Franck−Condon excited state while the distortions in medium frequency modes are consistent with $\gamma \approx 1.0$. In contrast, Figure 2 indicates that there is not only a far greater distortion in the low frequency vibrational modes of the emitting than of the Franck−Condon MLCT excited state for $[Os(bpy)_3]^{2+}$, but there is a significantly smaller distortion in the medium frequency vibrational modes (even assuming that $\gamma = 1.0$; see below). The contrasts in the observed and calculated vibronic sidebands are displayed more clearly in the difference spectra in Figure 3.

The 77 K emission emission maxima of the $[Os(d_8\text{-}bpy)_{3-n}(h_8\text{-}bpy)_n]^{2+}$ isotopomers are compared in Figure 4 and their spectra (in butyronitrile) are summarized in Supporting Information Table S8.

(32) Chen, Y.-J.; Endicott, J. F.; Swayambunathan, V. *Chem. Phys.* **2006**, *326*, 79.
(33) Based on a best fit value of g = 1.3.
(34) Chen, Y.-J.; Xie, P.; Endicott, J. F.; Odongo, O. S. *J. Phys. Chem. A* **2006**, *110*, 7970.

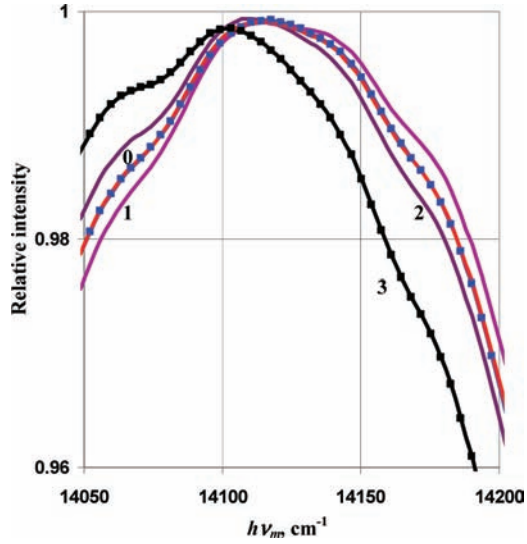

Figure 4. Comparison of the emission maxima of the $[Os(d_8\text{-bpy})_{3-n}(h_8\text{-bpy})_n]^{2+}$ complexes. For $n = 3$, black; $n = 2$, purple; $n = 1$, violet; $n = 0$, blue; average for $n = 0$ to $n = 2$, red (mean squared deviation <1%). These spectra have been smoothed.

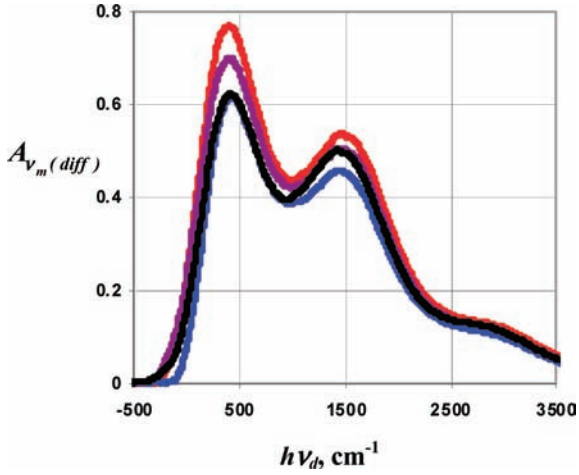

Figure 5. Comparison of the difference spectra of the $[Os(d_8\text{-bpy})_{3-n}(h_8\text{-bpy})_n]^{2+}$ complexes. For $n = 3$, black; $n = 2$, purple; $n = 1$, red; $n = 0$, blue; $h\nu_d = (h\nu_{max(f)} - h\nu_m)$.

Figure 4 indicates that the emission maxima of the $[Os(d_8\text{-bpy})_{3-n}(h_8\text{-bpy})_n]^{2+}$isotopomers where $n = 0-2$ are indistinguishable within our estimated uncertainties ($\sim \pm 10$ cm^{-1}). On the other hand, there is a significant blue shift of the emission of all of these complexes relative to $[Os(h_8\text{-bpy})_3]^{2+}$: 20 ± 10 cm^{-1} based on the emission maxima, and 34 ± 25 cm^{-1} based on $h\nu_{max(f)}$ for the deconvoluted fundamental components. The amplitudes of the low frequency vibronic components in the isotopomer difference spectra in Figure 5 are all larger than the medium frequency components which correspond mostly to distortions in bpy vibrational modes. These low frequency components fall in the range that is typical of metal−ligand vibrational modes.

If we assume that the experimental correlation between the sideband and the fundamental component amplitudes found for $[Ru(bpy)_3]^{2+}$ (i.e., for $\gamma = 1.0$ in eq 1) applies equally well to $[Os(bpy)_3]^{2+}$, then there are two limiting interpretations of the discrepancies between the observed spectrum and the rR parameters in the low frequency and medium frequency regimes:

(1) The rR parameters correctly describe distortions in the medium frequency (∼bpy) vibrational modes, but contributions of the low frequency components with the fundamental component overlap so much that our deconvolution procedure has overestimated $I_{max(f)}$, and Figures 3 and 5 greatly underestimate the low frequency contributions. Related problems have been previously encountered for the [Ru(1,4,7,10-tetraazacycloduodecane)bpy]$^{2+}$ complex and Ru-bpy complexes with halide ligands.[7,8]

(2) There is significantly less distortion in the medium frequency (∼bpy) vibrational modes in the emitting (and vibrationally equilibrated) excited state than in the Franck−Condon excited state.

We have attempted to fit the $[Os(bpy)_3]^{2+}$ spectrum to each of these limiting possibilities. However, the increased amplitudes of low frequency contributions required by spectral fittings in the first limit require corresponding increases in the amplitudes of the low frequency-medium frequency combination bands in the $h\nu_d = 1800-2000$ cm^{-1} region, and we have been unable to find values of $I_{max(f)}$ for which these combination band amplitudes are compatible with the observed spectrum. It seems likely that some combination of these two limiting cases would be more appropriate than is either limit alone, but we have no basis for constructing such a combination.

When the medium frequency vibronic contributions are removed from the difference spectra of $[Os(bpy)_3]^{2+}$, $[Ru(bpy)_3]^{2+}$, and $[Ru(NH_3)_4bpy]^{2+}$ the remaining low frequency components can be fitted to a progression in a single "equivalent" low frequency vibrational mode[8] for the systematic evaluations of the contrasts between the implications of the rR parameters and the spectroscopic observations shown in Figure 6 and Table 1. Thus, the integrated intensities of an emission spectral fit based on limit 2 above indicate that only 21% of the overall emission intensity is in the medium frequency vibronic components while 35% is in the fundamental.

Table 1 indicates that the observed low frequency contributions to the emission sidebands are often larger than expected based on rR parameters, and the discrepancies between the observed and calculated vibronic envelope amplitudes (based on the ratios I_{lf}/I_{mf}) decrease in the order $[Os(h_8\text{-bpy})_3]^{2+}$ (∼3600%) ≫ $[Ru(d_8\text{-bpy})_3]^{2+}$ (∼90%) > $[Ru(h_8\text{-bpy})_3]^{2+}$ (∼20−50%) > $[Ru(NH_3)_4bpy]^{2+}$ (∼0%).[33]

B. $[Ru(bpy)_3]^{2+}$ Emission Spectra. We have redetermined the $[Ru(bpy)_3]^{2+}$ emission spectrum for the conditions and spectrometer calibrations used in this study to minimize ambiguities in the comparisons of the Os and Ru complexes. Such comparisons are shown in Figures 2, 3, and 6. In contrast to Figure 1, the dominant medium frequency sideband in the $[Os(bpy)_3]^{2+}$ spectrum has a much smaller relative amplitude than that of the $[Ru(bpy)_3]^{2+}$ spectrum.

Discussion

The observed 77 K emission spectrum of $[Os(bpy)_3]^{2+}$ is dramatically different from that expected based on the

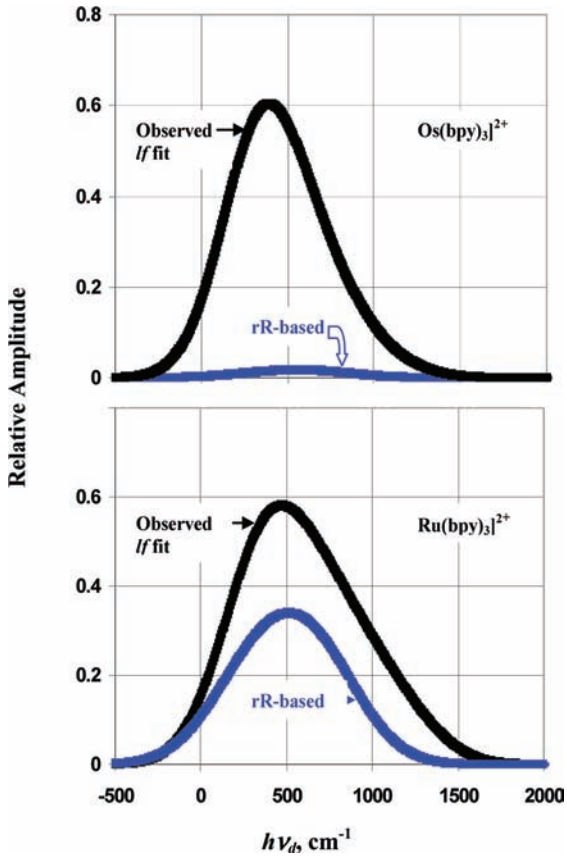

Figure 6. Comparison of the envelopes of low frequency ($h\nu_d$ < 800 cm^{-1}) vibronic components based on rR parameters[15,20] (blue curves) and found (black curves) in the 77 K CT emission spectra of $[Os(bpy)_3]^{2+}$ (top panel) and $[Ru(bpy)_3]^{2+}$ (bottom panel). The envelopes of the "observed" components are based on the best fit of a progression in a single "equivalent" low frequency mode to the spectral components that remain after accounting for contributions of the fundamental medium frequency modes are removed. Only the first order rR contributions have been included in the rR-based envelopes.

reported[20] rR parameters: (1) there are very large vibronic contributions in the low frequency regime; and (2) the amplitude of the envelope of medium frequency vibronic contributions is significantly smaller than expected. The contrasts between the observed and rR-based vibronic side bands are much greater than we found previously for $[Ru(bpy)_3]^{2+}$ or $[Ru(NH_3)_4bpy]^{2+}$.[8,9] We have previously suggested that most of the low frequency vibronic contributions in the Ru-bpy complex emission spectra arise from configurational mixing between the ^{3}MLCT and low ^{3}LF excited states,[7−9,34] and the large low frequency vibronic components found in the $[Os(bpy)_3]^{2+}$ emission are consistent with that hypothesis. On the other hand, the contrast between simple and seemingly straightforward fits of the $[Ru(bpy)_3]^{2+}$ 77 K emission spectrum to eq 1 (rR-based band shape functions, V_{ν_m}, with $\gamma = 1.0$)[7−9] and the smaller value of $\gamma = 0.7$ for the $[Os(bpy)_3]^{2+}$ emission spectrum, Figures 2 and 3, has been surprising. In evaluating this contrast, it is necessary to consider: (a) what would be expected of γ in some idealized limits; and (b) the properties of these systems that might possibly give rise to the observed features.

A. Some General Features of the Emission Spectra of These Multimode Systems and the Contrasts with Single Mode Approximations. Vibronic contributions are commonly treated using a Franck−Condon approach, and it is instructive to begin with a Franck−Condon treatment of the contributions that arise from distortions in a single vibrational mode. Such single mode treatments should at least qualitatively represent key elements of the basic physical issues, and they have often been used for this class of complexes.[20,23,35,36] The emission from an excited state that is distorted in a single vibrational mode may be represented as[37]

$$I_{\nu_m} = C(e^{-S_1}G_{0'0} + S_1e^{-S_1}G_1 + S_1^2e^{-S_1}G_{1+1} + ...) \quad (19)$$

Thus for eq 1 in this limit with $A_{max(f)} = 1.00$, $V_{\nu_m} = (S_1e^{-S_1}G_1 + S_1^2e^{-S_1}G_{1+1} + ...)$ and for $S_1 < \sim 1.5$, $\gamma_{FC} \approx e^{S_1}$ (see Supporting Information S5; note that in our recent paper we set $\gamma_{FC} = 1.0$ in our discussion of this model, but this is not correct for $S_1 > \sim 0.1$).[8] Possible fits of the $[Os(bpy)_3]^{2+}$ 77 K emission spectrum to this limit are shown in Figure 7 using (a) the value of $S_1 = 0.9$ reported[20] for the fits of the ambient spectrum; (b) a best fit of the 77 K spectrum using eq 19; and (c) a best fit of the 77 K spectrum assuming that the transition moment is frequency independent (e.g., see eq 4). These are all poor fits and even the best 77 K fit fails to account for the appreciable vibronic contributions in the low frequency regime. It is particularly notable that the maximum sideband amplitude based on the parameter $S_1 = 0.9$ reported for the fits to the ambient emission spectrum[20] exceeds the amplitude (S_1(77K) ~ 0.4) for the related single mode fit of the 77 K vibronic sideband by $\Delta S_1 \approx 0.5$. Very similar features are found for the single mode fits of the 77 K $[Ru(bpy)_3]^{2+}$ emission spectrum (Supporting Information-Figure S9). Among the possible contributions to ΔS_1 are (1) differences of component bandwidths and overlapping second order low frequency contributions at 77 and 300 K;[9] (2) temperature dependent changes in the populations of emitting MLCT excited states.[29,38−42]

Figure 8 indicates that ~40% of ΔS_1 arises from the differences in component bandwidths at 77 and 300 K and ~20% is the result of a difference in spectral scaling. Another 20% may result from the overlap of first order medium frequency and second order low frequency vibronic components. The remaining contributions could arise from a temperature dependence of the population of emitting excited-state components; this possibility is discussed below. The bandwidth dependencies of the $[Os(bpy)_3]^{2+}$ vibronic

(35) Caspar, J. V.; Kober, E. M.; Sullivan, B. P.; Meyer, T. J. *J. Am. Chem. Soc.* **1982**, *104*, 630.
(36) Thompson, D. W.; Fleming, C. N.; Myron, B. D.; Meyer, T. J. *J. Phys. Chem. B* **2007**, *111*, 6930.
(37) Myers, A. B.; Mathies, R. A.; Tannor, D. J.; Heller, E. J. *J. Chem. Phys.* **1982**, *77*, 3857.
(38) Elfring, W. H.; Crosby, G. A. *J. Am. Chem. Soc.* **1981**, *103*, 2683.
(39) Ferguson, J.; Krausz, E. *Inorg. Chem.* **1987**, *26*, 1383.
(40) Krausz, E.; Moran, G. *J. Lumin.* **1988**, *42*, 21.
(41) Braun, D.; Hensler, C.; Callhuber, E.; Yersin, H. *J. Phys. Chem.* **1991**, *95*, 1067.
(42) Yersin, H.; Strasser, J. *J. Lumin.* **1997**, *72*, 462.
(43) Endicott, J. F. In *Electron Transfer in Chemistry.*; Balzani, V., Ed.; Wiley-VCH: New York, 2001; Vol. 1; p 238.

Table 1. Best Fit Spectral Components for $[Os(bpy)_2]^{n+}$, $[Ru(bpy)_3]^{2+}$ and $[Ru(NH_3)_4bpy]^{2+}$[a]

complex	excited state	$h\nu_{max(abs)}$ (ambient)	$h\nu_{max(em)}$ (77 K)	$h\nu_{max(f)}$ ($\Delta\nu_{1/2}$)[b]	$h\nu_{dmax(lf)}$ [$I_{max(lf)}$] ($\Delta\nu_{1/2}$)[c]{basis}	$h\nu_{dmax(mf)}$ [$I_{max(mf)}$] ($\Delta\nu_{1/2}$)[d]	I_{lf}/I_{mf} [e]
$[Os(h_8\text{-bpy})_3]^{2+}$	Franck−Condon	20,810			553 [0.016] (708) {rR}[f]	1458 [0.52] (736) {rR}[f]	0.033
	emitting		14,095	14,200 (572)	390 [0.60] (520) {fit}	1454 [0.35][g] (736){rR}[f]	1.2 (1.5)[h]
$[Ru(h_8\text{-bpy})_3]^{2+}$	Franck−Condon	22,200			516 [0.34] (806) {rR}[i]	1387 [0.58] (748) {rR}[i]	0.6
	emitting		17,224	17,317 (629)	470 [0.58] (580) {fit}	1387 [0.58] (748) {rR}[i]	0.9 (0.73)[h]
$[Ru(d_8\text{-bpy})_3]^{2+}$	Franck−Condon				496 [0.35] (524) {rR}[i]	1417 [0.53] (700) {rR}[i]	0.5
	emitting [j]		17,225	17,330 (601)	411 [0.70] (480) {fit}	1417 [0.531] (700) {rR}[i]	0.9 (1.0)[h]
$[Ru(NH_3)_4bpy]^{2+}$ [i]	Franck−Condon	19,000			433 [0.48] (914) {rR}[k]	1416 [0.39] (976) {rR}[k]	1.2
	emitting [j]		12,394	12,440 (849)	498 [0.66] (790) {fit}[l]	1416 [0.54] (668) {rR}[k,l]	1.5 (1.7)[h,l]

[a] All energies in units of cm^{-1}; sideband intensities relative to $\gamma = 1.00$ for Ru complexes (except as noted) and $\gamma = 0.72$ for Os. Spectra determined in butyronitrile glasses at 77 K. [b] Gaussian parameters for the fundamental component deconvoluted from the 77 K emission spectrum. [c] Gaussian parameters based on rR of an "equivalent" single mode fit of the low frequency components that remain when the medium frequency rR components are subtracted from the difference spectrum {diff}. [d] Gaussian parameters for the envelope of 1st order medium frequency contributions based on reported rR parameters except as indicated. [e] $I_{pf} = I_{max(pf)} \times \Delta\nu_{1/2(pf)}$. [f] Resonance-Raman parameters from Thompson et al.[20] [g] Calculated from attenuated rR parameters. [h] For numerically integrated contributions of 1st order components to the intensities: $(\int_{-1000}^{1000} A_{\nu_m(lf;fit)} d\nu_d) \div (\int_{1000}^{4500} A_{\nu_m(rR;fit)} d\nu_d)$. [i] Resonance-Raman parameters from Maruszewski et al.[15] [j] Spectroscopic data from Xie et al.[9] [k] Resonance-Raman parameters from Hupp and Williams.[16] [l] Based on the best fit with $\gamma = 1.3$.

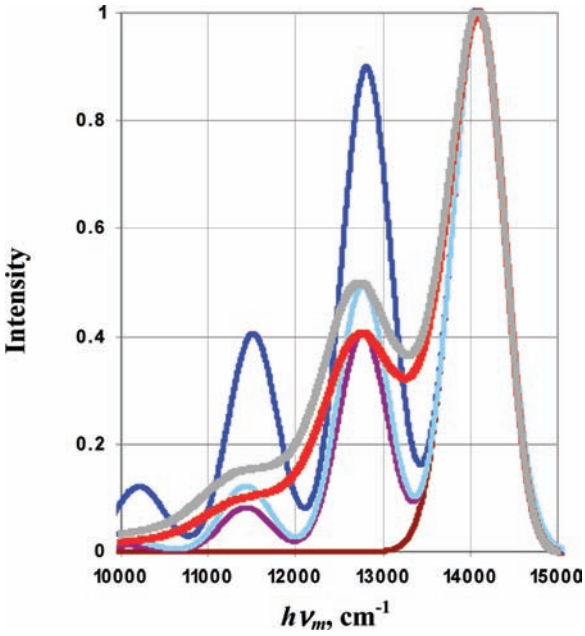

Figure 7. Single distortion mode fittings of the 77 K $[Os(bpy)_3]^{2+}$ emission spectrum (heavy red curve): $S = 0.90$, blue curve; $S = 0.49$, pale blue curve; $S = 0.40$, violet curve; fundamental component, dark red Gaussian. The gray curve was constructed from the experimental emission spectrum assuming that the transition moment rather than the electronic matrix element (as assumed for the red curve) is independent of ν_m. The fundamental component in this figure is constructed to account for most of the intensity of the dominant emission feature, even though this does not fit the high energy side of the emission spectrum very well.

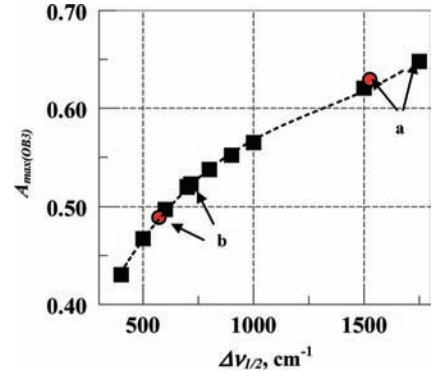

Figure 8. Variations in the maximum amplitudes (at ~1440 cm^{-1}) of envelopes of medium frequency vibronic components with variations in component bandwidths as calculated from rR parameters of $[Os(bpy)_3]^{2+}$. The bandwidths for the ambient[20,37] (a) and 77 K (based on I_{ν_m} constructed as in Figure 7) (b) single mode fittings for the $[Os(bpy)_3]^{2+}$ (red points) and $[Ru(bpy)_3]^{2+}$ (indicated black points) emissions are indicated by the arrows.

envelopes based on rR parameters are shown in Supporting Information S10.[24]

B. Some Considerations of Excited-State Energies. The excited-state energies for charge transfer systems can to some degree be approximated by their differences in standard oxidation and reduction potentials, $F\Delta E_{1/2}$ (e.g., see eqs 13 and 14 and Supporting Information S7), and the energies of CT absorption and emission maxima generally correlate with $F\Delta E_{1/2}$.[31,43,44] Figure 9, which compares $h\nu_{max(abs)}$ and $h\nu_{max(em)}$ for $[Os(bpy)_3]^{2+}$ with the spectral-electrochemical correlation found previously for the $[Ru(Am)_{6-2n}(bpy)_n]^{2+}$ complexes (Am = an am(m)ine),[7−9] indicates that both the MLCT absorption and emission of the Os complex are higher in energy than expected by at least 2,000 cm^{-1}. A possible origin for this contrast is that there is more MLCT/ground-state configurational mixing for the Os complex than for the Ru complexes. Such an increase in configurational mixing is a likely consequence of the approximately three times greater spin−orbit coupling in Os than Ru complexes;[44,45] hence, the more intense ground state ^{3}MLCT absorbance (see Supporting Information Figure S3).[24] The deviations in properties of the emitting MLCT excited state, which has nominal triplet spin multiplicity, from those expected in a diabatic limit can be expressed in terms of the configurational mixing between (1) the ground state and the MLCT excited states to reduce the amount of excited-state distortion; and (2) between the lowest energy MLCT excited state and other excited states to introduce distortions that are unique to the higher energy excited states (such as in the metal ligand vibrational modes for metal centered excited states).[7−9,14,18,19,25,34,46,47]

The dramatic contrast between the insignificant low frequency contributions found in the rR spectra[20,41] of

(44) Gorelsky, S. I.; Kotov, V. Y.; Lever, A. B. P. *Inorg. Chem.* **1998**, *37*, 4584.
(45) D'Alessandro, D. M.; Dinolfo, P. H.; Hupp, J. T.; Davies, M. S.; Keene, F. R. *Inorg. Chem.* **2006**, *45*, 3261.
(46) Chen, Y.-J.; McNamara, P. G.; Endicott, J. F. *J. Phys. Chem. B* **2007**, *111*, 6748.
(47) Endicott, J. F.; Schegel, H. B.; Uddin, M. J.; Seneviratne, D. *Coord. Chem. Rev.* **2002**, *229*, 95.
(48) Nozaki, K.; Takamori, K.; Nakatsugawa, Y.; Ohno, T. *Inorg. Chem.* **2006**, *45*, 6161.

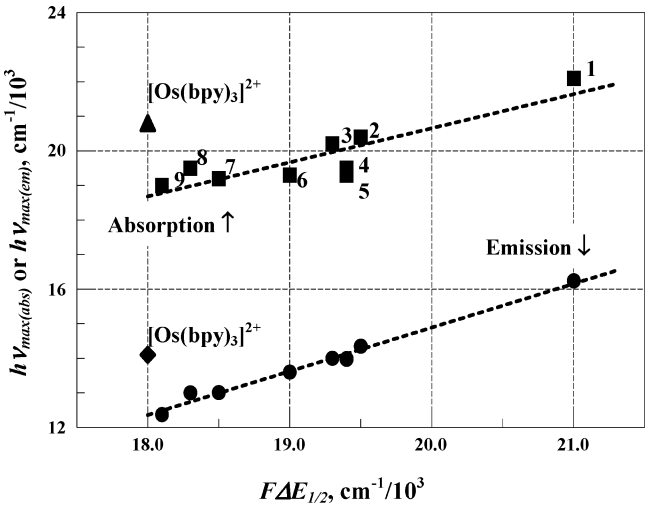

Figure 9. Contrasts in the relationship of the ambient MLCT absorption and 77 K emission maxima to the differences in complex oxidation and reduction potentials for $[Os(bpy)_3]^{2+}$ (triangle and diamond, respectively) and the $[Ru(Am)_{6-2n}(bpy)_n]^{2+}$ (squares and circles, respectively; data from ref 7) complexes. The Ru complexes are numbered for absorption and follow the same sequence for emission. For $[Ru(bpy)_3]^{2+}$, 1. For the other Ru complexes $(Am)_{6-2n}$ (n): en (2), 1; $(NH_3)_2$ (2), 3; *rac*-Me_6[14]aneN_4 (1), 4; [14]aneN_4 (1), 5; [15]aneN_4 (1), 6; $(en)_2$ (1), 7; trien (1), 8; $(NH_3)_4$ (1), 9. The least-squares lines for the $[Ru(Am)_{6-2n}(bpy)_n]^{2+}$ data are (absorption) $h\nu_{max(abs)} = (0.98 \pm 0.20)(F\Delta E_{1/2}) + (0.9 \pm 3.8)$ ($r^2 = 0.8$); and (emission) $h\nu_{max(em)} = (1.27 \pm 0.06)(F\Delta E_{1/2}) - (10 \pm 1)$ ($r^2 = 0.99$).

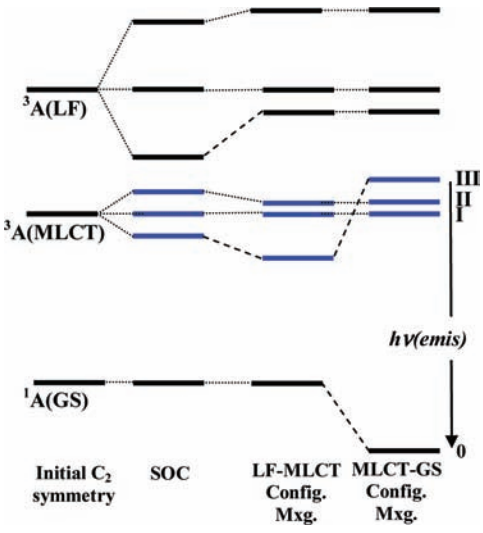

Figure 10. Qualitative scheme illustrating the possible effects of configurational mixing and spin−orbit coupling (SOC) on the lowest energy ^{3}MLCT and ^{3}LF excited states in the localized limit (C_2) and a homogeneous environment. The lines representing the spin−orbit components of the ^{3}MLCT excited state are in blue for clarity.

$[Os(bpy)_3]^{2+}$ and their dominant contributions to the emission spectra, indicates that there is much more configurational mixing of the metal centered excited states with the lowest energy MLCT excited states than with the Franck−Condon excited state. This could be a consequence of a larger spin−orbit splitting of the ^{3}LF than the ^{3}MLCT excited states. A simple, qualitative scheme illustrating such configurational mixings is presented in Figure 10.

C. Implications of the Observed Bandshapes. Since the rR probes the Franck−Condon excited state, which must have D_3 symmetry in $[M(bpy)_3]^{2+}$ complexes, and since the lowest energy vibrationally relaxed MLCT excited state could have C_2 symmetry if electron density were localized on a single ligand in the excited state, some of the band shape contrasts could be related to a difference in the excited-state symmetries. However, a recent DFT study has suggested that the lowest energy excited state of $[Os(bpy)_3]^{2+}$ always has D_3 symmetry while that of the Ru complex usually has C_2 symmetry.[48] Perdeuteration of the bpy ligands results in a smaller zero point energy of the $[M(d_8\text{-bpy})_3]^{2+}$ than the $[M(h_8\text{-bpy})_3]^{2+}$ complex in either the ground or the excited state by an amount that is proportional to about $0.3h\nu_{CH}$, and the zero point energy of an MLCT excited state in which an electron is localized on a d_8-bpy ligand is smaller than that of the corresponding excited state with an electron localized on a h_8-bpy ligand so that proportionately more electron density will reside on the d_8-bpy ligands than the h_8-bpy ligands of the mixed ligand isotopomers ($n = 1$ or 2) even if the electron is delocalized when all the ligands have the same isotopic composition (i.e., for $n = 0$ or $n = 3$).[49] However, the observation that perdeuteration of the bpy ligands results in a blue shift of the $[Os(bpy)_3]^{2+}$ emission (20 ± 10 cm^{-1} in $h\nu_{max(em)}$ and 34 ± 10 cm^{-1} in $h\nu_{max(f)}$), comparable to that found for the $[Ru(bpy)_3]^{2+}$ complex,[34,50] and that the blue shifts are independent of whether the $[Os(d_8\text{-bpy})_{3-n}(h_8\text{-bpy})_n]^{2+}$ isotopomers contain one, two or three d_8-bpy ligands (Figure 3) is indicative of electron localization and C_2 symmetry in the MLCT excited states of these substrates in frozen solutions. There is a small but systematic variation in the isotopomer emission bandshapes: (a) the isotopomers with identical ligands ($n = 0$ or 3) have indistinguishable vibronic bandshapes; while (b) the low frequency vibronic contributions of the mixed ligand isotopomers are larger than either of these and greater for $n = 1$ than for $n = 2$ (see Figure 3). These differences in vibronic amplitudes may indicate that the ratio $A_{max(lf)}/A_{max(mf)}$ increases as the electron density becomes more localized on a single ligand (i.e., as the contribution of the low symmetry structure increases), but the effect is small (~15% in the ratio and ~20% in $A_{max(lf)}$) and these observations are complicated by differences in bandwidth and uncertainties in deconvoluting $I_{\nu_m(f)}$ so their significance is not clear. In view of these observations, the Franck−Condon and emitting excited states probably do differ in symmetry, and such a symmetry difference would imply that there are more constraints on configurational mixing in the Franck−Condon than in the emitting MLCT excited state. In addition, the metal centered excited states are expected to have much higher energies in the Os than in the Ru complex, so that the combination of the symmetry constraints in the Franck−Condon excited state and the excited-state energy differences could account for the very small amplitude Huang−Rhys parameters reported

(49) Riesen, H.; Wallace, L.; Krausz, E. *J. Chem. Phys.* **1995**, *102*, 4823.
(50) Yersin, H.; Braun, D. *Chem. Phys. Lett.* **1991**, *179*, 85.
(51) The sums of the first order Huang-Rhys parameters reported for the two ruthenium complexes are 1.103 and 0.769, respectively. The first of these is not consistent with the condition that $\gamma = (1 - \sum_k S_k e^{-S_k})^{-1}$; this suggests that there may be a difference in the bandwidths for low and medium frequency vibronic components and/or there is a problem with parameter normalization. For the osmium complex, $\sum_k S_k e^{-S_k} = 0.61$ and is consistent with expectation. See Supporting Information S1 and S5.

for low frequency vibrational modes of the $[Os(bpy)_3]^{2+}$ complex.[20] We will assume that the vibrationally equilibrated ($[M(bpy)_3]^{2+}$ ^{3}MLCT excited states have C_2 symmetry in the 77 K frozen solutions.

The considerations in section A above bring into focus an issue that we have overlooked in our earlier studies: Our experimental correlations of the rR based vibronic bandshapes, V_{ν_m}, with the observed 77 K emission spectra of $[Ru(bpy)_3]^{2+}$ and $[Ru(NH_3)_4bpy]^{2+}$ implied that $\gamma_{expt} \approx 1.0$ in eq 1, whereas a Franck−Condon model for the vibronic band shape would require that $\gamma_{FC} \geq \sim\exp(\sum_k S_k e^{-S_k})$, analogous to the value of γ_{FC} inferred from eq 19 (see Supporting Information S5).[24,51] The sums of reported Huang−Rhys parameters for these two complexes imply that most of the emission intensity is in the vibronic components contrary to observation (see Supporting InformationTable S5A).[24,52] Similarly, even if only first order terms are considered to contribute to the intensity, the rR parameters imply that (1) the medium frequency modes contribute about 3−4 times as much as the band origin component to the intensity of the emission spectrum contrary to observations (the observed ratio is about 0.21/0.35 = 0.6/1; Supporting InformationTable S5A);[24] and (2) $\gamma_{FC} \gg \exp(\sum_k S_k e^{-S_k}) =$ 1.8 (based on rR parameters; see Figure S5C)[24] for $[Os(bpy)_3]^{2+}$ while our observations indicate that $\gamma_{expt} \sim 0.7$. Thus, in the systems so far examined, $\gamma_{FC} \gg \gamma_{expt}$, and this discrepancy might result from some problem with our approach to evaluating the emission bandshapes, some issue with the reported displacement amplitudes or from some intrinsic physical properties of the complexes. Two possible ways of fitting the rR parameters to the observed $[Os(bpy)_3]^{2+}$ emission spectrum are compared in Figure 11 (see Supporting Information S11 for the comparable comparisons for $[Ru(bpy)_3]^{2+}$).[24]

It is possible that our experimental estimate of $I_{\nu_m(f)}$ is in error as a result of overlap with low frequency vibronic contributions but such contributions would have to have very large amplitudes (i.e., more than six times larger than our estimates) to account for the observed spectra, and this could result in an even larger value for γ_{FC}. Since there is no experimental evidence for the required huge distortions in low frequency vibrational modes of the complexes considered here, a very large error of this sort can be discounted.

We have adjusted the Franck−Condon-like vibronic fitting (B) in Figure 11 to fit the medium frequency vibronic sideband and to minimize the differences with the fundamental component that is deconvoluted from the experimental spectrum. Although this Franck−Condon "progression" does not provide a good fit of the observed spectrum, it does illustrate some important points: (1) even setting $\gamma = \exp(0.72\sum_k S_k e^{-S_k})$ results in a fundamental component whose amplitude is much smaller than is required to fit the spectrum (the use of unattenuated rR parameters lead to a value that has only 40% of the amplitude of the deconvoluted fundamental component); (2) the procedure that we have used in Figure 11 provides an upper limit for $A_{max(f)}$(FC) (see

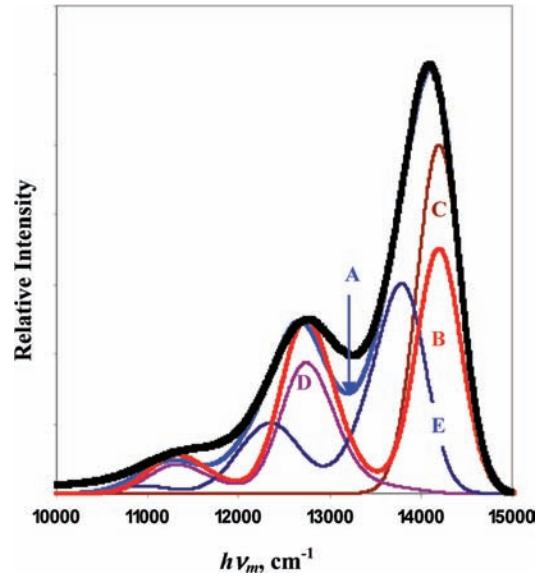

Figure 11. Comparison of the observed 77 K emission spectrum of $[Os(bpy)_3]^{2+}$ (black curve) and those calculated from (A) an optimized fit (blue curve); and (B) an expectation based on a Franck−Condon progression in rR-based medium frequency modes (red curve). The fitting employed (1) a best fit fundamental component (dark red curve, C); (2) an envelope of medium frequency components based on 28% attenuation of rR parameters so that $\gamma = 1.0$ (violet curve, D); and (3) a best fit progression in single low frequency vibronic component (dark blue curve, E). The fit based on rR parameters (B) is based on (1) the attenuated medium frequency, rR-based components (2, above); (2) assuming that the fraction of emission in the band origin component is $A_{max(f)} \approx \exp(-0.72\sum_k S_k e^{-S_k}) \approx 0.65$; but (3) adjusted the maximum amplitude of the medium frequency sideband to fit the corresponding amplitude of the emission spectrum which results in $A_{max(f)}(FC) = 0.70$ (i.e., ∼70% that of the original fundamental component). The fitting of the fundamental component for B has not been optimized for the different values of γ and does not include additional vibronic contributions in the low frequency regime. Parameters for the fitting A are listed in Supporting Information Table S8.[24]

Supporting Information Figures S5B and S5C);[24] (3) significant low frequency vibronic components are necessary to fit the 77 K emission spectrum (see Figures 7 and 11). Very similar features are found in attempting a Franck−Condon-based fitting of the rR parameters to the $[Ru(bpy)_3]^{2+}$ emission spectrum (see Supporting Information Figure S11).[24]

This comparison of the vibronic sidebands observed in the 77 K emission to those calculated from rR parameters suggests that there are differences in the distortions of the ^{1}MLCT and ^{3}MLCT excited states. Possible origins of such differences are (1) differences in configurational mixing with other electronic states in the singlet and triplet manifolds; and/or (2) differences in the distortions in the spin orbit components of the triplet states.[29,41,52] As noted above and previously,[7,9,18,19,32,53] configurational mixing with the ground state does have significant consequences for observed excited-state energies and bandshapes as is illustrated by the significantly smaller medium frequency vibronic sidebands[9] and Huang−Rhys parameters reported for $[Ru(NH_3)_4bpy]^{2+}$ [16] than for either $[Ru(bpy)_3]^{2+}$ [15] or $[Os(bpy)_3]^{2+}$.[20] If we assume that the attenuation is the same in all of the distortion modes and in the limit that

(52) Yersin, H.; Humbs, W.; Strasser, J. *Coord. Chem. Rev.* **1997**, *159*, 325.
(53) Endicott, J. F.; Chen, Y.-J. *Inorg. Chim. Acta* **2007**, *360*, 913.
(54) Lever, A. B. P.; Gorelsky, S. I. *Coord. Chem. Rev.* **2000**, *208*, 153.

the extent of mixing is small ($\alpha_{jk}^2 < 0.1$, where $\alpha_{jk} \cong H_{jk}/(E_{jk}[1 + (H_{jk}/E_{jk})^2]^{1/2})$ is a normalized mixing coefficient and E_{jk} is the vertical energy difference between the states j and k) so that for spin allowed transitions ($\{g,v\} \rightarrow \{e,v'\}$) and using the notation from eq 1,

$$V_{\nu_m(a)} \approx V^o_{\nu_m}(1 - 2\alpha^2_{ge} - 2\alpha^2_{eg}) \quad (20)$$

where $V^o_{\nu_m}$ is the band shape function in the diabatic limit (no configurational mixing) and the mixing coefficients are evaluated for the nuclear coordinates of the ground state (α_{ge}) or excited state (α_{eg}) potential energy minima. However, different parameters are required if the emission corresponds to a different electronic state (designated e^*), even assuming that the diabatic band shape functions are the same, so that,

$$V_{\nu_m(e^*)} \approx V^o_{\nu_m}(1 - 2\alpha^2_{ge} - 2\alpha^2_{e^*g}) \quad (21)$$

Thus, a band shape function inferred from the ^{1}MLCT excited-state manifold may be approximately related to that applicable in the ^{3}MLCT manifold by

$$V_{\nu_m(e^*)} \approx \frac{V_{\nu_m(a)}(1 - 2\alpha^2_{ge} - 2\alpha^2_{e^*g})}{1 - 2\alpha^2_{ge} - 2\alpha^2_{eg}} \approx V_{\nu_{m(a)}}(1 + 2\alpha^2_{eg} - 2\alpha^2_{e^*g} + ...) \quad (22)$$

Equations 20−22 imply that when there is MLCT/ground-state configurational mixing, the observed vibronic components of these complexes are all significantly smaller in amplitude than would be the case for the diabatic limit. When $E_{eg} = E_{e^*g}$, $\alpha_{eg} > \alpha_{e^*g}$ for the ^{3}MLCT/ground-state mixing, but the large exchange energies that are characteristic of these complexes,[54] which require that $E_{eg} > E_{e^*g}$, and spin−orbit coupling will lead to significant values for H_{jk} to somewhat moderate the inequality in mixing coefficients. Nevertheless, it seems likely that in most cases that ground state/MLCT excited-state configurational mixing leads to somewhat more attenuation of the distortion in the ^{1}MLCT than in the ^{3}MLCT excited state so that the amplitude of $V_{\nu_m(e^*)}$ will tend to be greater than that of $V_{\nu_m(a)}$ in the limit that the diabatic band shape functions are the same in the two states. Configurational mixing with higher energy electronic excited states will have related effects, and some additional attenuation of bpy distortion modes is to be expected in the M-bpy complexes when there is appreciable mixing with ligand field excited states; however, we have not yet found any distinct patterns of vibronic attenuation with the amplitudes of low frequency vibronic contributions in this class of complexes, and we do not have a means of assessing such effects at this time.

The zero-field splitting of the lowest energy ^{3}MLCT excited states of these complexes is potentially a simple and important interpretation of the observation that $\gamma_{FC} \gg \gamma_{expt}$ since the resulting electronic excited-state components have been found to have different emission characteristics.[29,38−42] Thus, zero-field splitting components (designated as I−V) have been identified for $[Ru(bpy)_3]^{2+}$ in single crystal matrixes,[29,38−40,42] and the states II, III, IV, and V have zero point energies of approximately 8.7, 61, 150, and 800 cm^{-1}, respectively, greater than that of state I.[29,42] It should be noted that in the localized C_2 limit, a "^{3}MLCT" configuration in a homogeneous environment can only have three spin−orbit excited-state components (as in Figure 10), while the orbital degeneracy may be greater and more components are possible for a "^{3}MLCT" configuration in the D_3 limit. In a rigid medium, there can be more than three near in energy ^{3}MLCT excited-state components even in a localized limit if the molecular environments of the bpy ligands are not identical; such environmental differences can arise from crystal site symmetry or partial relaxation of a glass upon cooling of the Franck−Condon excited state. For the component energies reported for $[Ru(bpy)_3]^{2+}$,[29,43] the origins of states I−III (and possibly IV) would all be convoluted into our fundamental component at 77 K. Of these states, I is very weakly emissive and its vibronic components do not correlate with the rR spectra[29] so it would not contribute to values of γ_{expt}. The remaining states apparently do exhibit Franck–Condon vibronic progressions in vibrational modes that correspond to rR frequencies.[29] If the distortions of the states II-IV are different, then the extent to which they are populated will contribute to variations in γ_{expt}. Such differences in distortions may result in variations of their relative energies as a result of differences in their solvent matrix stabilization, configurational mixing with other excited states or some other factors as illustrated in Figure 10 for the idealized C_2 limit. The related zero-field splittings for $[Os(bpy)_3]^{2+}$ are larger, and states II and III have energies that are approximately 63, and 211 cm^{-1}, respectively, relative to that of state I in crystalline matrixes.[41,42] This difference could be related to the smaller value of γ_{expt} found for $[Os(bpy)_3]^{2+}$.[41] If this behavior is a result of the zero field splittings of the ^{3}MLCT excited state, then γ_{expt} could range from a very small low temperature limit to a high temperature limit of γ_{FC}. These considerations suggest that the normalized amplitudes of the vibronic sidebands (V_{ν_m}; for constant $\Delta\nu_{1/2}$) for this class of complexes could be temperature dependent and that they will not generally conform to the expectations of a simple Franck−Condon model. On the other hand, there may be other intrinsic differences in the distortions of the MLCT excited state singlet and triplet manifolds that lead to the observations that $V^o_{max}(\text{singlet}) > V^o_{max}(\text{triplet})$, but this is not clear at this time.

Conclusions

In summary, the spectroscopy of the $[Os(bpy)_3]^{2+}$ complex illustrates many of the challenges in attempts to characterize structural variations in the lowest energy excited states of transition metal complexes. Since these tend to be the photoreactive excited states, and since chemical reactivity is determined by a combination of structural and electronic contributions, such characterization is essential in the design of complexes that optimize the efficiencies of photoinduced processes. The inference that the ^{3}MLCT excited-state is less distorted at 77 K than is the ^{1}MLCT excited-state at 300 K raises the possibility that its zero field splitting results in several near in energy excited state components which differ significantly in their distortions and therefore in their patterns

of electron-transfer reactivity. This feature would make complexes of this class unique photoelectron transfer reagents since (1) the zero field splitting components would be in labile equilibrium on the picosecond time frame; (2) the lowest energy ^{3}MLCT component with very small distortions states would have very small intrinsic reorganizational barriers for normal region electron transfer to external reagents (more or less comparable to those of their ground states); (3) the distorted higher energy components states should have appreciable intrinsic reorganizational barriers for normal region electron transfer but should provide relatively facile electron transfer pathways in the Marcus inverted region.

Acknowledgment. The authors thank the Office of Basic Energy Sciences of the Department of Energy and the Office of the Vice President for Research of Wayne State University for partial support of this research.

Supporting Information Available: Comparison of resonance Raman parameters; synthetic details; absorption spectra; half-wave potentials of the complexes; relative component amplitudes; fitting procedures used for emission spectra; basis for correlation of spectral and electrochemical parameters; spectral components for some $[M(bpy)_3]^{2+}$ complexes; single distortion mode fittings of the 77 K $[Ru(bpy)_3]^{2+}$ emission spectrum; medium frequency vibronic envelopes calculated from rR parameters of $[Os(bpy)_3]^{2+}$; comparison of the observed 77 K emission spectrum of $[Ru(bpy)_3]^{2+}$ and spectra calculated from rR parameters; temperature dependence of the ratio of vibronic to fundamental component amplitudes. This material is available free of charge via the Internet at http://pubs.acs.org.

IC801512G